

Fragmentation dynamics of electron-impact double ionization of helium

Shiwei Liu(刘士炜), Difa Ye(叶地发), and Jie Liu(刘杰)

Citation: Chin. Phys. B, 2023, 32 (**6**): 063402. DOI: 10.1088/1674-1056/acbe33
Journal homepage: http://cpb.iphy.ac.cn; http://iopscience.iop.org/cpb

What follows is a list of articles you may be interested in

Development of an electronic stopping power model based on deep learning and its application in ion range prediction

Xun Guo(郭寻), Hao Wang(王浩), Changkai Li(李长楷),Shijun Zhao(赵仕俊), Ke Jin(靳柯), and Jianming Xue(薛建明)

Chin. Phys. B, 2022, 31 (**7**): 073402. DOI: 10.1088/1674-1056/ac4e0c

Multiple recollisions in nonsequential double ionization below the recollision-ionization threshold

Xiao-Meng Ma(马晓萌), Ai-Hong Tong(童爱红), Zhuo Wang(王茁), and Chun-Yang Zhai(翟春洋)

Chin. Phys. B, 2021, 30 (**12**): 123402. DOI: 10.1088/1674-1056/ac2d1e

Evidence of potential change in nonsequential double ionization

Changchun Jia(贾昌春), Pu Zhang(张朴), Hua Wen(文华), and Zhangjin Chen(陈长进)

Chin. Phys. B, 2021, 30 (**2**): 023401. DOI: 10.1088/1674-1056/abc151

Surface for methane combustion: $O(^3P)+CH_4 \rightarrow OH+CH_3$

Ya Peng(彭亚), Zhong-An Jiang(蒋仲安), Ju-Shi Chen(陈举师)

Chin. Phys. B, 2020, 29 (**7**): 073401. DOI: 10.1088/1674-1056/ab90f5

Dynamics of the $CH_4+O(^3P) \rightarrow CH_3(v=0)+OH(v'=0)$ reaction

Zhong-An Jiang(蒋仲安), Ya Peng(彭亚), Ju-Shi Chen(陈举师), Gui Lan(兰桂), Hao-Yu Lin(林浩宇)

Chin. Phys. B, 2018, 27 (**6**): 063401. DOI: 10.1088/1674-1056/27/6/063401

SPECIAL TOPIC — Celebrating the 100th Anniversary of Physics Discipline of Xiamen University

Fragmentation dynamics of electron-impact double ionization of helium

Shiwei Liu(刘士炜)[1], Difa Ye(叶地发)[1,2,†], and Jie Liu(刘杰)[3,4,‡]

[1] *Beijing Computational Science Research Center, Beijing* 100193, *China*
[2] *Laboratory of Computational Physics, Institute of Applied Physics and Computational Mathematics, Beijing* 100088, *China*
[3] *Graduate School, China Academy of Engineering Physics, Beijing* 100193, *China*
[4] *HEDPS, Center for Applied Physics and Technology, and College of Engineering, Peking University, Beijing* 100871, *China*

(Received 11 January 2023; revised manuscript received 5 February 2023; accepted manuscript online 23 February 2023)

We study the double ionization dynamics of a helium atom impacted by electrons with full-dimensional classical trajectory Monte Carlo simulation. The excess energy is chosen to cover a wide range of values from 5 eV to 1 keV for comparative study. At the lowest excess energy, i.e., close to the double-ionization threshold, it is found that the projectile momentum is totally transferred to the recoil-ion while the residual energy is randomly partitioned among the three outgoing electrons, which are then most probably emitted with an equilateral triangle configuration. Our results agree well with experiments as compared with early quantum-mechanical calculation as well as classical simulation based on a two-dimensional Bohr's model. Furthermore, by mapping the final momentum vectors event by event into a Dalitz plot, we unambiguously demonstrate that the ergodicity has been reached and thus confirm a long-term scenario conceived by Wannier. The time scale for such few-body thermalization, from the initial nonequilibrium state to the final microcanonical distribution, is only about 100 attoseconds. Finally, we predict that, with the increase of the excess energy, the dominant emission configuration undergoes a transition from equilateral triangle to T-shape and finally to a co-linear mode. The associated signatures of such configuration transition in the electron–ion joint momentum spectrum and triple-electron angular distribution are also demonstrated.

Keywords: double ionization, classical trajectory Monte Carlo simulation, Wannier threshold law, ergodicity

PACS: 34.10.+x, 34.80.–i, 34.50.Fa **DOI:** 10.1088/1674-1056/acbe33

1. Introduction

Electron-impact ionizations of atoms and molecules are, on one hand, fundamental processes to understand the electron correlation in nature, and on the other hand, empowering versatile applications ranging from microelectronics fabrication,[1] human healthcare,[2] to astrophysical diagnosis.[3,4] Here, of particular interest is the low-energy scattering processes close to the ionization threshold, which, for example, was found to be the dominant mechanism in biomolecular damage of DNA under external radiations.[5,6] It is even envisaged that, in the near future, with a high flux of low-energy electrons, radiation-based targeted cancer therapies might become possible.[7]

During the past decades, the understanding of low-energy collision processes has been significantly advanced by sophisticated measurements with cold target recoil ion momentum spectroscopy (COLTRIMS) in experiment[8] and, complementarily in theory, by the development and application of state-of-the-art quantum-mechanical approaches,[9] e.g., the convergent close coupling (CCC),[10] time-dependent close-coupling (TDCC),[11] R-matrix with pseudo-states (RMPS),[12] and exterior complex scaling (ECS) methods.[13] One should note, however, it is until recently that the simplest four-body breakup process, i.e., electron-impact double-ionization of helium (He) at low impact energies close to ionization threshold, can be solved numerically with massive parallel supercomputers, e.g., using roughly 30000 cores on a Cray XC40 with a total of 216 h of wall-clock time.[14] The dynamics of even more complex multi-electron quantum systems is still an open question. To this point of view, it is highly desirable to develop feasible classical or semiclassical models,[15] which are also beneficial to other related fields such as particle simulation of warm dense plasmas physics[16] and material science.[17]

Electron-impact double-ionization of He, as one of the simplest four-body breakup processes, has attracted great attention during the past years, both theoretically and experimentally. The research interest can be dated back to Wannier's one-page seminal work,[18] in which the famous Wannier threshold law[19,20] was extended from single ionization to multiple ionization of atoms. The Wannier theory is constituted by three pillars: the ergodic hypothesis, the scaling law of ionization cross section, and the final emission configuration. For $e + He \rightarrow He^{2+} + 3e$, the threshold law is predicted to be $\sigma \propto E_{exc}^{n}$, with the system excess energy

†Corresponding author. E-mail: ye_difa@iapcm.ac.cn
‡Corresponding author. E-mail: jliu@gscaep.ac.cn

© 2023 Chinese Physical Society and IOP Publishing Ltd

$E_{\rm exc} = E - E_{\rm threshold}$ and the exponent n slightly larger than 2, which has been confirmed in an experiment as early as in 1968[21] and later refinements.[22,23] It is only until recently, however, a more thorough analysis, e.g., on the angular distributions for three ejected electrons, has become possible in the kinematically complete experiment with coincidence measurements.[24–26] As an example, it was shown that for a total excess energy of 5 eV, the three slow continuum electrons in the final state should most probably be emitted with the equilateral triangle configuration, i.e., the relative angles between each pair of the electrons are all 120°.[25] This is in accordance with analysis on the saddle points of the asymptotic Hamiltonian[27] but contradicts an earlier detailed classical trajectory simulation where a T-shape emission was predicted even if the excess energy penetrated down to 2 eV.[28] Furthermore, in a recent delicate TDCC calculation,[14] the angular distribution was found to peak at an angle slightly lower than 120°. Thus, the situation that there exist significant discrepancies between experiments and theories, either *ab-initio* quantum-mechanical simulation or the classical modeling, needs further clarification. Last but not least, the cornerstone of Wannier's theory, i.e., the ergodic hypothesis, has so far escaped rigorous tests.

In this work, we reexamine the ergodicity in electron-impact double-ionization of He by close inspection of the momentum transfer between the break-up ion and electrons as well as the energy sharing and the angular correlation among the three outgoing electrons. This is facilitated by the classical trajectory Monte Carlo (CTMC) approach[29–31] adopting a Heisenberg potential to prevent non-physical autoionization of a classical multi-electron atom.[32–34] With simulations of a large ensemble of classical trajectories, we unambiguously demonstrate the signature of ergodicity when the electron impact energy is close to the double-ionization threshold of He. Furthermore, it is confirmed that the dominant emission geometry of the three outgoing electrons in the close-to-threshold region is the symmetric configuration predicted by Wannier's theory, in good agreement with an early experiment.[25] We then further extend the simulations to several higher excess energies and reveal a transition of the dominant emission configurations.

The paper is organized as follows. In Section 2, we introduce the CTMC model. Our simulation results are presented and discussed in Section 3. Section 4 concludes the paper. Atomic units (a.u.) are used throughout the paper unless otherwise specified.

2. Model

The use of the CTMC approach in studying atomic collisions can be dated back to the early 1960s as introduced by Abrines and Percival,[35] and then further extended by Olson *et al.* to electron impact ionization (see, e.g., Ref. [36]). It has also become a powerful tool in studying the laser-driven ionization dynamics of atoms and molecules,[29–32] as well as laser-assisted atomic collisions[33,34] and nuclear processes,[37,38] etc.

In CTMC, the electrons are treated as classical point particles and the initial momenta and positions of the bound electrons are sampled from a micro-canonical ensemble with fixed total energy. The coupled classical equations of motion can be easily solved in a three-dimensional framework, taking full account of the Coulomb potentials between electrons and nuclei as well as electrons and electrons. However, a multi-electron classical atom can be unstable, suffering nonphysical autoionization due to the absence of the lower bounds on the electron energies imposed by quantum mechanics. To circumvent this problem, Kirschbaum and Wilets proposed a momentum-dependent effective two-body potential

$$V_{\rm H}(\boldsymbol{r},\boldsymbol{p}) = \frac{\xi^2}{4\alpha|\boldsymbol{r}|^2}\exp\left\{\alpha\left[1-\left(\frac{|\boldsymbol{r}||\boldsymbol{p}|}{\xi}\right)^4\right]\right\} \tag{1}$$

to mimic the Heisenberg uncertainty principle which prevents the electron from visiting parts of the classical phase space that would be forbidden in quantum mechanics.[39] Here, the position and momentum of the electron are denoted by $\boldsymbol{r}$ and $\boldsymbol{p}$, respectively. The parameter α controls the rigidity of the Heisenberg core and ξ is chosen to fit the atomic or ionic binding energy for a given α.[40–44]

Considering that the mass of the nucleus is much larger than that of the electrons, the total classical Hamiltonian of an electron–helium scattering system can be written as

$$\begin{aligned} H =& \sum_{i=1}^{3}\left(\frac{\boldsymbol{p}_i^2}{2}-\frac{1}{|\boldsymbol{r}_i|}\right)+\sum_{i,j=1;i<j}^{3}\frac{1}{|\boldsymbol{r}_i-\boldsymbol{r}_j|} \\ &+\sum_{i=1}^{3}\frac{\xi^2}{4\alpha\boldsymbol{r}_i^2}\exp\left\{\alpha\left[1-\left(\frac{|\boldsymbol{r}_i||\boldsymbol{p}_i|}{\xi}\right)^4\right]\right\}, \end{aligned} \tag{2}$$

where $i = 1$, 2, and 3 denote the three active electrons, including two bound electrons of the helium atom and one incident electron. In our simulations, the incident electrons propagate along the z axis starting from a position (e.g., $z_{\rm in} = -50$ a.u.) far away from the helium atom. They are uniformly distributed in a circular disk parallel to the Oxy plane. The center of the disk is on the z axis, and its radius is set as 2 a.u., large enough to ensure the convergence of the statistical cross section.

The ground state of the helium atom is defined as the particle configuration which minimizes the value of the Hamiltonian

$$\begin{aligned} H_0 =& \frac{\boldsymbol{p}_1^2}{2}+\frac{\boldsymbol{p}_2^2}{2}-\frac{1}{|\boldsymbol{r}_1|}-\frac{1}{|\boldsymbol{r}_2|}+\frac{1}{|\boldsymbol{r}_1-\boldsymbol{r}_2|} \\ &+\frac{\xi^2}{4\alpha\boldsymbol{r}_1^2}\exp\left\{\alpha\left[1-\left(\frac{|\boldsymbol{r}_1||\boldsymbol{p}_1|}{\xi}\right)^4\right]\right\} \end{aligned}$$

$$+\frac{\xi^2}{4\alpha r_2^2}\exp\left\{\alpha\left[1-\left(\frac{|\boldsymbol{r}_2||\boldsymbol{p}_2|}{\xi}\right)^4\right]\right\}.$$

The rigid parameter α is set as 5, and ξ is chosen to fit the binding energy of He^+, which gives $\xi = 0.9535$. By adding another electron and employing the minimization algorithm detailed in Refs. [41,45], we then obtain the ground state configuration of the helium atom, whose total energy is equal to -3.0625 a.u., a little bit ($\sim 5\%$) lower than the experimental value -2.9 a.u., but such a minor discrepancy does not change the physical picture we show later. The position and momentum of the electron in the ground state are $|\boldsymbol{r}_1| = |\boldsymbol{r}_2| = 0.5714$ a.u. and $|\boldsymbol{p}_1| = |\boldsymbol{p}_2| = 1.6685$ a.u., respectively. The two electrons locate co-linearly with the nucleus sitting in the center. With this given configuration and employing the Monte Carlo sampling technique to make random Euler's rotation of the positions and momenta independently,[46] we finally get a microcanonical ensemble of the helium atom.

The dynamics of the electron–helium system is governed by the following canonical equations:

$$\frac{\mathrm{d}\boldsymbol{r}_i}{\mathrm{d}t} = \frac{\partial H}{\partial \boldsymbol{p}_i}, \quad \frac{\mathrm{d}\boldsymbol{p}_i}{\mathrm{d}t} = -\frac{\partial H}{\partial \boldsymbol{r}_i}. \tag{3}$$

They are solved numerically by employing the standard 4-5th Runge–Kutta algorithm and the double ionization events are identified by the final energy of the three electrons, all greater than zero. More than 10^6 classical electron trajectories are traced for each different projectile energy of the incident electron, giving rise to at least 10^4 double ionization events for further statistics.

3. Results and analysis

3.1. Momentum transfer

We simulate the double ionization process of helium impacted by electron over a wide span of excess energies $E_{\mathrm{exc}} = E - E_{\mathrm{threshold}}$ ranging from 5 eV to 1 keV. Here E is the incident energy carried by the projectile electron and $E_{\mathrm{threshold}}$ is the minimal energy required to doubly ionize the helium atom. We first show how the momentum carried by the incident electron is partitioned among three electrons and the nucleus during the process of double ionization.

To this end, we first calculate the initial momentum of the incident electron according to $\boldsymbol{p}_0 = \sqrt{2E}\boldsymbol{e}_z$ and the final momenta $\boldsymbol{p}_i$ ($i = 1$, 2, and 3) of the three electrons by numerically solving Newton's equation. Then the momentum of the recoil-ion He^{2+} can be obtained according to the conservation law of momentum,

$$\boldsymbol{p}_{\mathrm{ion}} = \boldsymbol{p}_0 - \boldsymbol{p}_{\mathrm{sum}} = \boldsymbol{p}_0 - (\boldsymbol{p}_1 + \boldsymbol{p}_2 + \boldsymbol{p}_3), \tag{4}$$

with $\boldsymbol{p}_{\mathrm{sum}} = \boldsymbol{p}_1 + \boldsymbol{p}_2 + \boldsymbol{p}_3$ the sum momentum of the three receding electrons. The results are shown in Fig. 1. Here, in order to guide the eyes, we have added two dash lines in each sub plot, one is $p_{z,\mathrm{sum}} = 0$ (left dash line in Fig. 1) and the other $p_{z,\mathrm{ion}} = \sqrt{2E}$ (right dash line in Fig. 1) representing all the initial incident momentum is transferred to the recoil-ion. Meanwhile, two circles centered at (0, 0) and $(\sqrt{2E}, 0)$ with radius $\sqrt{2E_{\mathrm{exc}}}$ are also presented. These circles give a constraint on the maximal momentum (or equivalently, energy) retained to redistribute among the three electrons after the incident electron transferring just enough energy to release the two bound electrons of the helium atom.

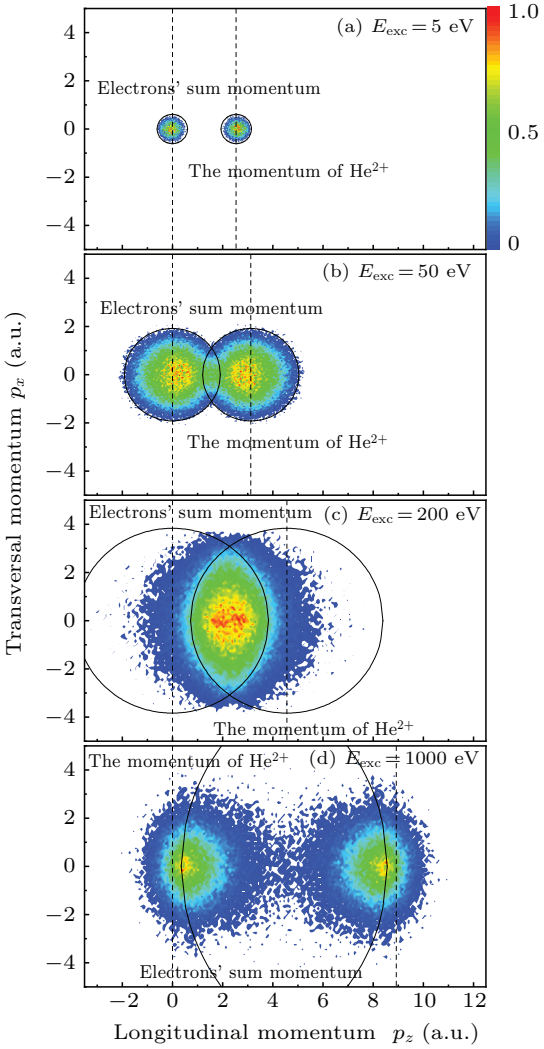


Fig. 1. The electron–ion joint momentum distribution of double ionization events at different excess energies. The two circles centered at (0, 0) and $(\sqrt{2E}, 0)$ with radius $\sqrt{2E_{\mathrm{exc}}}$ give constraints on the final longitudinal and transversal momenta of the ion and electrons, according to conservation laws of energy and momentum (see text for details).

At the lowest incident energy we have considered, $E_{\mathrm{exc}} = 5$ eV [Fig. 1(a)], $p_{z,\mathrm{sum}}$ peaks around zero and $p_{z,\mathrm{ion}}$ peaks around 2.55 a.u., roughly equals to $\sqrt{2E}$. Moreover, the spread of the distribution is constrained within the maximal momentum, a final-state electron can gain $p_{\mathrm{max}} = \sqrt{2E_{\mathrm{exc}}} \approx 0.61$ a.u. For this near-threshold energy, all three final continuum electrons share the residual excess energy. However, none of them has an energy higher than $E_{\mathrm{exc}} = 5$ eV and, thus, cannot carry

momentum more than 0.61 a.u. Since the projectile electron loses most of its kinetic energy, the incident momentum is almost completely transferred to the recoil-ion. This physical picture is consistent with recent experimental observations.[25]

With increasing the excess energy to $E_{\rm exc} = 50$ eV [Fig. 1(b)], $p_{z,\rm sum}$ still peaks around zero but with a slight shift towards the projectile forward direction, while the width of the distribution is constrained within $\sqrt{2E_{\rm exc}} \approx 1.92$ a.u., as expected. This is because, accompanied by the increase of the incident energy, one of the outgoing electrons preferentially carries a larger part of the excess energy and is emitted more toward the forward direction shifting $\boldsymbol{p}_{\rm sum}$ accordingly.[25] Going further to even higher excess energy $E_{\rm exc} = 200$ eV [Fig. 1(c)], the distributions of $\boldsymbol{p}_{\rm ion}$ and $\boldsymbol{p}_{\rm sum}$ almost completely overlap. This indicates the even sharing of the projectile momentum between the electrons and the nucleus. Finally, when the excess energy increases up to $E_{\rm exc} = 1$ keV [Fig. 1(d)], $p_{z,\rm sum}$ reversely peaks around $\sqrt{2E}$ while $p_{z,\rm ion}$ peaks around zero, in sharp contrast to the low excess energy case close to the threshold, suggesting a completely different fragmentation dynamics. At this extremely high impact energy, one can assume that the lost energy of the projectile electron during the scattering process is roughly equal to the ionization energy of the helium atom.[47] Then the momentum transfer is only about 0.3 a.u., much smaller than the absolute value of the incident momentum (~ 8.9 a.u.). As a result, the projectile electron still dashes forward as revealed by the red spot on the right-hand side of Fig. 1(d).

3.2. Energy sharing

In the proceeding sub-section, we have demonstrated that, at the lowest excess energy close to the threshold, the projectile momentum is totally transferred to the recoil-ion. However, due to the large mass of the nucleus, its accumulated kinetic energy is indeed quite small. As a result, almost all the residual energy is shared by the three outgoing electrons, i.e., $T_1 + T_2 + T_3 \approx E_{\rm exc}$, where $T_i = \boldsymbol{p}_i^2/2$ ($i = 1$, 2, and 3) are the kinetic energy of the three electrons, respectively.

Wannier[18] has ever conceived that this energy conservation condition indeed constitutes a triangular segment in the three-dimensional space spanned by the respective kinetic energies.[48] The area of the triangle, and thus the number of kinetically allowed states, increases as the square of the excess energy. With the ergodic hypothesis that all these states are evenly occupied during the ionization process, the threshold law of ionization cross section then becomes the nth power. For an independent particle situation, n is exactly equal to two. The true exponent, however, is supposed to be slightly larger than two due to the electron–electron correlation.

To test this idea, we present the energy sharing of the three outgoing electrons in the Dalitz plot[49] as shown in Fig. 2. Here, the momentum vectors are mapped event by event into the coordinates of $(\varepsilon_2 - \varepsilon_3)/\sqrt{3}$ and $\varepsilon_1 - 1/3$, in which $\varepsilon_i = T_i/(T_1 + T_2 + T_3)$ is the relative energy (final state kinetic energy of each electron as a fraction of the total energy) of the three outgoing electrons, respectively.

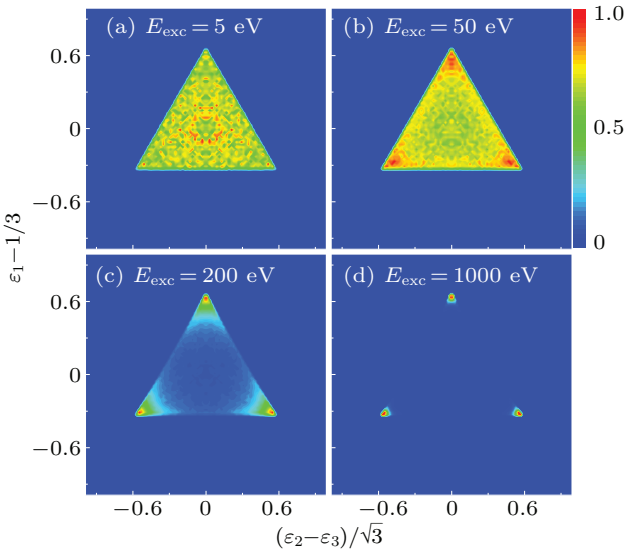


Fig. 2. Dalitz plot of the energy sharing of three outgoing electrons at the excess energies of 5 eV (a), 50 eV (b), 200 eV (c), and 1 keV (d), respectively.

At $E_{\rm exc} = 5$ eV [Fig. 2(a)], we find that the Dalitz plot is full of the entire triangular space, showing an almost random distribution. This suggests that, via few-body Coulomb interaction, the excess energy is distributed arbitrarily among the three outgoing electrons, as anticipated in Wannier's theory.[18,48] However, with the increase of the excess energy from $E_{\rm exc}$ = 50 eV to 1 keV [Figs. 2(b)–2(d)], the energy-sharing distribution in the Dalitz plot gradually concentrates to the three corners of the triangle. This can be explained by the fact that, at higher impact energies, the projectile electron tends to escape with more energy while the other two electrons are allocated just enough energy to escape.

3.3. Angular correlation

The triple-electron angular correlations between the final state continuum electrons are shown in Fig. 3 at different excess energies. Here θ_{ij} $(i, j = 1, 2, 3)$ represents the angle in between the momentum vectors of two arbitrarily chosen final-state electrons. For $E_{\rm exc} = 5$ eV, there exists a maximum at $\theta_{ij} = 120^\circ$ indicating the dominance of the equilateral triangle emission configuration. This is in accordance with the spirit of Wannier's theory which assumes that the mutual escape of several electrons from the ionic potential is only possible if their radial distances from the parent ion remain nearly equal. The minimization of the electrons' mutual repulsion results in particular angular configurations, e.g., an equilateral triangle for the three-electron escape. This

is supported by some quantum-mechanical calculations and a delicate experiment.[25] However, early classical trajectory simulations have predicted, down to 2 eV excess energy, a T-shape emission configuration in which two electrons were emitted back-to-back and the third one perpendicular to the other two.[28] This early classical model did not correctly predict the experimental observations probably because it was based on a two-dimensional (2D) Bohr's model that was unstable with respect to auto-ionization due to the absence of the lower bounds on the electron energies imposed by quantum mechanics. This difficulty is now solved by applying the Heisenberg potential to reconstruct the classical Hamiltonian.

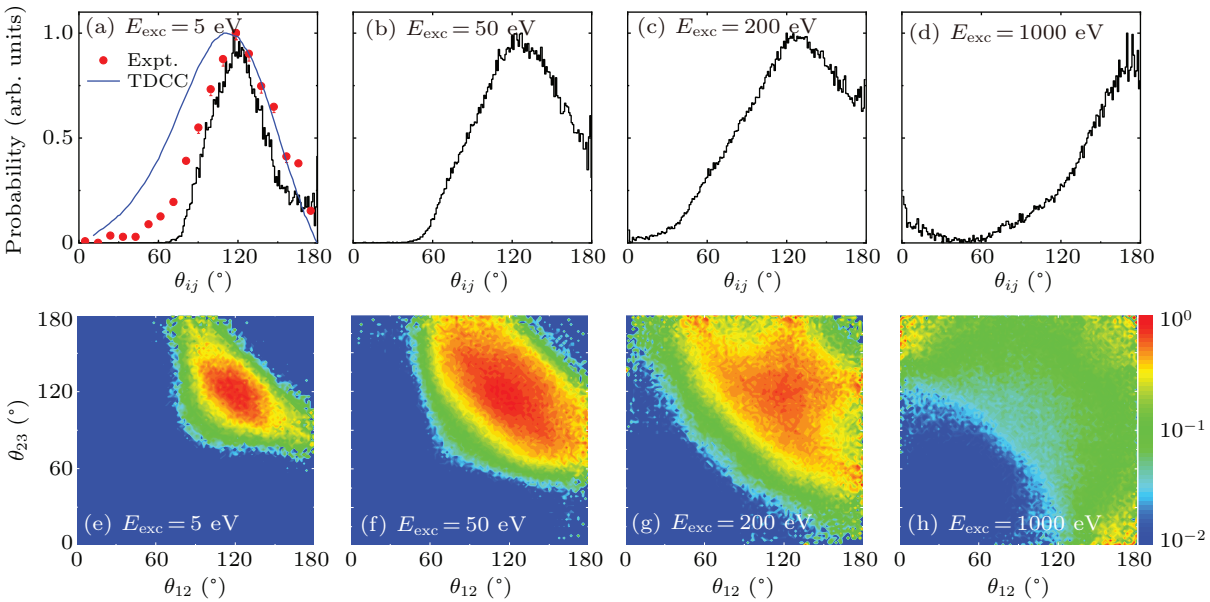


Fig. 3. (a)–(d) The distributions for the relative emission angles of the final-state electrons, where θ_{ij} $(i,j=1,2,3)$ represents the angle in between the momentum vectors of two arbitrarily chosen outgoing electrons. In this representation, the solid-angle correction factor $(\sin\theta_{ij})^{-1}$ is taken into account. In (a), the experimental measurements by Ren *et al.*[25] are denoted by red dots. The blue curve represents TDCC calculations by Colgan and Pindzola.[14] (e)–(h) The triple-electron angular correlations between the outgoing electrons at different excess energies. In this representation, the correction factor $(\sin\theta_{12}\times\sin\theta_{23})^{-1}$ is applied.

With the increase of the excess energy to $E_{\rm exc}=50$ eV [Fig. 3(b)] and 200 eV [Fig. 3(c)], the distribution still peaks at $\theta_{ij}=120°$. However, the relative contribution from $\theta_{ij}=180°$ becomes more and more significant, indicating the gradual enhancement of T-shape emission, in qualitative agreement with the experimental observations.[25] Finally, when the excess energy climbs up to $E_{\rm exc}=1$ keV [Fig. 3(d)], the dominant emission configuration becomes the co-linear mode peaking at $\theta_{ij}=180°$. This indicates that two of the three outgoing electrons are emitted back-to-back while the emission direction of the third electron is the same as one of the former two electrons. Actually, as revealed by the typical classical trajectories, the incident electron in this case preferentially carries a larger part of the excess energy after the double-ionization of He and is emitted more towards the forward direction.

3.4. Attosecond thermalization

In this sub-section, we present some typical trajectories to unravel the complex dynamics of the four-body break-up process. In Figs. 4(a) and 4(b), at $E_{\rm exc}=5$ eV, the typical emission configuration is equilateral triangle. We can see that at such near-threshold energy, the projectile electron first collides with one of the bound electrons, handing over most of its kinetic energy via few-body Coulomb interaction, and on its way out of the atomic core, encountering another bound electron. Finally, the excess energy is arbitrarily distributed among the three continuum electrons. If the energies of the three outgoing electrons are uniform and their sum momentum is equal to zero, they will be emitted in the same plane and the relative angles between them are all 120°. This is consistent with the experimental observations of Ref. [25]. As witnessed by Fig. 4(b), the typical time scale from the projectile electron coming close to the bound electrons to the redistribution of the excess energy and final burst out takes only about 100 attoseconds (3 a.u.).

Figures 4(c) and 4(d) demonstrate the typical trajectory of the T-shape emission when the residual excess energy is 50 eV. In this case, the incident electron also losses most of its kinetic energy to dislodge the bound electrons. However, the sum momentum of the three outgoing electrons $p_{z,\rm sum}$ does not peak at zero. This is because the incident electron still moves forward after momentum transfer to the recoil-ion and the bound electrons, while the two continuum electrons released from the helium atom break up back-to-back and perpendicular to the projectile, which gives rise to the so-called T-shape emission. Moving to even higher residual excess energy 1 keV [see Figs. 4(e) and 4(f)], the co-linear emission configuration starts to dominate. Here, the incident energy is so large that the

projectile electron hardly changes its direction during the scattering process. When the incident electron passes through the target atom, the two bound electrons will be mutually shaken off back-to-back, aligning along the incident direction.

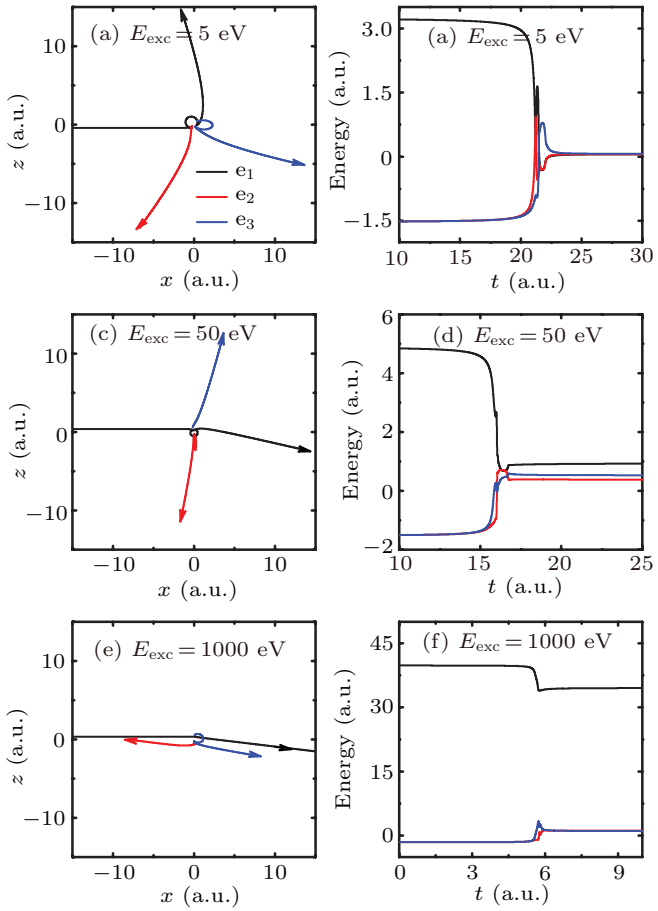


Fig. 4. Typical trajectories of double ionization at different excess energies. The left panel demonstrates the trajectories in the position space, while the right panel illustrates the corresponding energy evolution. For clear visualization, we have restricted the trajectories on a plane.

4. Conclusions

We have thoroughly investigated the double ionization dynamics of a helium atom impacted by electrons, over a rather wide span of excess energies ranging from 5 eV to 1 keV, and have identified the dominant physical mechanisms taking full advantage of the classical trajectory diagnosis. Our simulations have consolidated Wigner's picture, in particular, the ergodic hypothesis, on the fragmentation configuration of multiple ionization when the electron impact energy is close to the ionization threshold. The simulations successfully explained some early experiments. Finally, we have also predicted some new features on the dominant emission configuration with the excess energy of the projectile electrons increase. The associated signatures in the electron–ion joint momentum spectrum and triple-electron angular distribution were presented. These predictions are observable with the current experimental apparatus. We hope our work would stimulate further experiments. Furthermore, the method adopted in this paper can be extended to other more complex atomic,[41] molecular,[17,43] or even plasmas[16] systems. For a multi-electron target, the Pauli exclusion effects among the electrons might become significant. In this case, another type of effective potential, sometimes dubbed "Pauli potential", is required to model the electron–electron interaction.[15] It would be an interesting issue to study how the Pauli exclusion effects will affect the fragmentation dynamics in the future.

Acknowledgements

Project supported by the National Natural Science Foundation of China (Grant Nos. 12174034, 12047510, and 11822401) and NSAF (Grant Nos. U1930402 and U1930403).

References

[1] Bartschat K and Kushner M J 2016 *Proc. Natl. Acad. Sci. USA* **113** 7026
[2] Alizadeh E, Orlando T M and Sanche L 2015 *Annu. Rev. Phys. Chem.* **66** 379
[3] Güsten R, Wiesemeyer H, Neufeld D, Menten K M, Graf U U, Jacobs K, Klein B, Ricken O, Risacher C and Stutzki J 2019 *Nature* **568** 357
[4] Novotný O, Wilhelm P, Paul D, Kálosi Á, Saurabh S, Becker A, Blaum K, George S, Göck J, Grieser M, Grussie F, von Hahn R, Krantz C, Kreckel H, Meyer C, Mishra P M, Muell D, Nuesslein F, Orlov D A, Rimmler M, Schmidt V C, Shornikov A, Terekhov A S, Vogel S, Zajfman D and Wolf A 2019 *Science* **365** 676
[5] Michael B D and O'Neill P 2000 *Science* **287** 1603
[6] Boudaïffa B, Cloutier P, Hunting D, Huels M A and Sanche L 2000 *Science* **287** 1658
[7] Gokhberg K, Kolorenč P, Kuleff A I and Cederbaum L S 2014 *Nature* **505** 661
[8] Ullrich J, Moshammer R, Dorn A, Dörner R, Schmidt L Ph H and Schmidt-Böcking H 2003 *Rep. Prog. Phys.* **66** 1463
[9] Bray I, Fursa D V, Kadyrov A S, Stelbovics A T and Kheifets A S 2012 *Phys. Rep.* **520** 135
[10] Bray I, Bray A W, Fursa D V and Kadyrov A S 2018 *Phys. Rev. Lett.* **121** 203401
[11] Colgan J, Emmanouilidou A and Pindzola M S 2013 *Phys. Rev. Lett.* **110** 063001
[12] Burke P G 2011 *R-matrix Theory of Atomic Collisions* (New York: Springer)
[13] Rescigno T N, Baertschy M, Isaacs W A, McCurdy C W 1999 *Science* **286** 2474
[14] Colgan J and Pindzola M S 2018 *J. Phys. B* **51** 185202
[15] Feldmeier H and Schnack J 2000 *Rev. Mod. Phys.* **72** 655
[16] Su J T and Goddard III W A 2007 *Phys. Rev. Lett.* **99** 185003
[17] Senftle T P, Hong S, Islam M M, Kylasa S B, Zheng Y X, Shin Y K, Junkermeier C, Engel-Herbert R, Janik M J, Aktulga H M, Verstraelen T, Grama A and van Duin A C T 2016 *Npj Comput. Mater.* **2** 15011
[18] Wannier G H 1955 *Phys. Rev.* **100** 1180
[19] Wannier G H 1953 *Phys. Rev.* **90** 817
[20] Duan B, Bai Z Q and Gu Y 2000 *Acta Phys. Sin.* **49** 1428 (in Chinese)
[21] Brion C E and Thomas G E 1968 *Int. J. Mass Spectrom. Ion Phys.* **1** 25
[22] Lebius H, Koslowski H R, Wiesemann K and Huber B A 1991 *Ann. Phys. (Leipzig)* **503** 103
[23] Denifl S, Gstir B, Hanel G, Feketeova L, Matejcik S, Becker K, Stamatovic A, Scheier P and Märk T D 2002 *J. Phys. B* **35** 4685
[24] Dürr M, Dorn A, Ullrich J, Cao S P, Czasch A, Kheifets A S, Götz J R and Briggs J S 2007 *Phys. Rev. Lett.* **98** 193201
[25] Ren X, Dorn A and Ullrich J 2008 *Phys. Rev. Lett.* **101** 093201
[26] Cao S P, Ma X W, Dorn A, Dürr M and Ullrich J 2007 *Acta Phys. Sin.* **56** 6386 (in Chinese)
[27] Klar H and Schlecht W 1976 *J. Phys. B* **9** 1699
[28] Dimitrijevic M S and Grujic P 1981 *J. Phys. B* **14** 1663
[29] Liu J 2013 *Classical Trajectory Perspective of Atomic Ionization in Strong Laser Fields: Semiclassical Modeling* (New York: Springer)

[30] Ye D F, Liu X J and Liu J 2008 *Phys. Rev. Lett.* **101** 233003
[31] Ye D F, Li M, Fu L B, Liu J, Gong Q H, Liu Y Q and Ullrich J 2015 *Phys. Rev. Lett.* **115** 123001
[32] Yuan J Y, Liu S W, Wang X C, Shen Z J, Ma Y X, Ma H Y, Meng Q X, Yan T M, Zhang Y Z, Dorn A, Weidemüller M, Ye D F and Jiang Y H 2020 *Phys. Rev. A* **102** 043112
[33] Liu S W, Ye D F and Liu J 2020 *Phys. Rev. A* **101** 052704
[34] Liu S W, Ye D F and Liu J 2020 *J. Phys. B: At. Mol. Opt. Phys.* **53** 145005
[35] Abrines R and Percival I C 1966 *Proc. Phys. Soc. London* **88** 861
[36] Olson R E and Gay T J 1988 *Phys. Rev. Lett.* **61** 302
[37] Liu S W, Duan H, Ye D F and Liu J 2021 *Phys. Rev. C* **104** 044614
[38] Liu S W, Ye D F and Liu J 2022 *Phys. Rev. C* **106** 064611
[39] Kirschbaum C L and Wilets L 1980 *Phys. Rev. A* **21** 834
[40] Zajfman D and Maor D 1986 *Phys. Rev. Lett.* **56** 320
[41] Cohen J S 1995 *Phys. Rev. A* **51** 266
[42] Zhou Y M, Huang C, Liao Q and Lu P X 2012 *Phys. Rev. Lett.* **109** 053004
[43] Lötstedt E, Kato T and Yamanouchi K 2011 *Phys. Rev. Lett.* **106** 203001
[44] Zhou J and Wang X 2022 *Opt. Express* **30** 16802
[45] Nelder J A and Mead R 1965 *Comput. J.* **7** 308
[46] Cohen J S 1982 *Phys. Rev. A* **26** 3008
[47] Lahmam-Bennani A, Duguet A, Gaboriaud M N 2001 *J. Phys. B* **34** 3073
[48] Read F H 1985 *Threshold behavior of ionization cross-sections*, in *Electron Impact Ionization*, edited by Märk T D and Dunn G H (New York: Springer-Verlag)
[49] Dalitz R H 1953 *Philos. Mag.* **44** 1068